Published Online: 10 March, 1997 | Supp Info: http://doi.org/10.1083/jcb.136.5.995
Downloaded from jcb.rupress.org on November 11, 2019

Inner but Not Outer Membrane Leaflets Control the Transition from Glycosylphosphatidylinositol-anchored Influenza Hemagglutinin-induced Hemifusion to Full Fusion

Grigory B. Melikyan, Sofya A. Brener, Dong C. Ok, and Fredric S. Cohen

Department of Molecular Biophysics and Physiology, Rush Medical College, Chicago, Illinois 60612

Abstract. Cells that express wild-type influenza hemagglutinin (HA) fully fuse to RBCs, while cells that express the HA-ectodomain anchored to membranes by glycosylphosphatidylinositol, rather than by a transmembrane domain, only hemifuse to RBCs. Amphipaths were inserted into inner and outer membrane leaflets to determine the contribution of each leaflet in the transition from hemifusion to fusion. When inserted into outer leaflets, amphipaths did not promote the transition, independent of whether the agent induces monolayers to bend outward (conferring positive spontaneous monolayer curvature) or inward (negative curvature). In contrast, when incorporated into inner leaflets, positive curvature agents led to full fusion. This suggests that fusion is completed when a lipidic fusion pore with net positive curvature is formed by the inner leaflets that compose a hemifusion diaphragm. Suboptimal fusion conditions were established for RBCs bound to cells expressing wild-type HA so that lipid but not aqueous dye spread was observed. While this is the same pattern of dye spread as in stable hemifusion, for this "stunted" fusion, lower concentrations of amphipaths in inner leaflets were required to promote transfer of aqueous dyes. Also, these amphipaths induced larger pores for stunted fusion than they generated within a stable hemifusion diaphragm. Therefore, spontaneous curvature of inner leaflets can affect formation and enlargement of fusion pores induced by HA. We propose that after the HA-ectodomain induces hemifusion, the transmembrane domain causes pore formation by conferring positive spontaneous curvature to leaflets of the hemifusion diaphragm.

In protein-mediated membrane fusion, lipids reorient from two bilayers into one (White, 1992). Thus, lipids must temporarily leave the bilayer arrangement for a nonbilayer formation. Nonbilayer structures are known to be favored by certain lipids (Tilcock and Cullis, 1987; Seddon, 1990). For example, phosphatidylethanolamine and *cis*-unsaturated fatty acids, with head group areas small compared with tails, have shapes referred to as "cone shapes." They promote formation of the H_{II} phase (a negative curvature surface) and favor fusion (Tilcock and Cullis, 1987; Epand et al., 1991). In contrast, lysophosphatidylcholine (LPC)[1], with its single acyl chain and large area headgroup, has the shape of an "inverted cone" (Tilock and Cullis, 1987). Inverted cone–shaped amphipaths pack to form micelles (a positive curvature surface) (Epand, 1985) and inhibit fusion when inserted in external leaflets in a wide variety of protein-mediated fusion systems, including fusion mediated by hemagglutinin (HA) of influenza virus (Vogel et al., 1993; Chernomordik et al., 1995*b*; Günther-Ausborn et al., 1995; Shangguan et al., 1996). These results suggest that the initial structure connecting membranes has a net negative curvature. The simplest structure, requiring the fewest lipids to reorient, is a "stalk," a local and transient "hourglass"-shaped nonlamellar formation (Fig. 1, *stalk*) that joins the external, facing monolayers of apposed membranes (Kozlov et al., 1989; Siegel, 1993; Chernomordik et al., 1995*a*). When the stalk forms, the membranes become locally hemifused. Hemifusion is the merger of outer monolayers without the mixing of inner monolayers or formation of fusion pores. The expansion of a stalk, promoted by cone-shaped lipids (Kozlov et al., 1989), brings the inner, distal monolayers into contact and a hemifusion diaphragm (HD) forms (Fig. 1, *hemifusion*). In this model, fusion is completed when a pore forms within the HD (Fig. 1, *fusion*). If hemifusion is, in fact, a universal intermediate stage, it would explain how fusion can occur in a vast number of disparate systems without leakage of aqueous contents.

The shape of lipids may be critical not only for outer

Address all correspondence to Fredric S. Cohen, Department of Molecular Biophysics and Physiology, Rush Medical College, 1653 W. Congress Parkway, Chicago, IL 60612. Tel.: (312) 942-6753. Fax: (312) 942-8711. e-mail: fcohen@rpslmc.edu

1. *Abbreviations used in this paper*: CF, 6-carboxyfluorescein; CPZ, chlorpromazine; M-CPZ, metho-chlorpromazine; DB, dibucaine; DOPC, dioleoylphosphatidylcholine; DOPE, dioleoylphosphatidylethanolamine; GPI, glycosylphosphatidylinositol; HA, hemagglutinin; HD, hemifusion diaphragm; LPC, lysophosphatidylcholine; L-LPC, lyso-lauroylphosphatidylcholine; S-LPC, lyso-stearoylphosphatidylcholine; MPCA, membrane-permeable, cationic amphipaths; NBD-t, NBD-taurine; PS, phosphatidylserine; RD, tetramethylrhodamine-dextran; R18, octadecylrhodamine B chloride; TFP, trifluoperazine; WT, wild type.

© The Rockefeller University Press, 0021-9525/97/03/995/11 $2.00

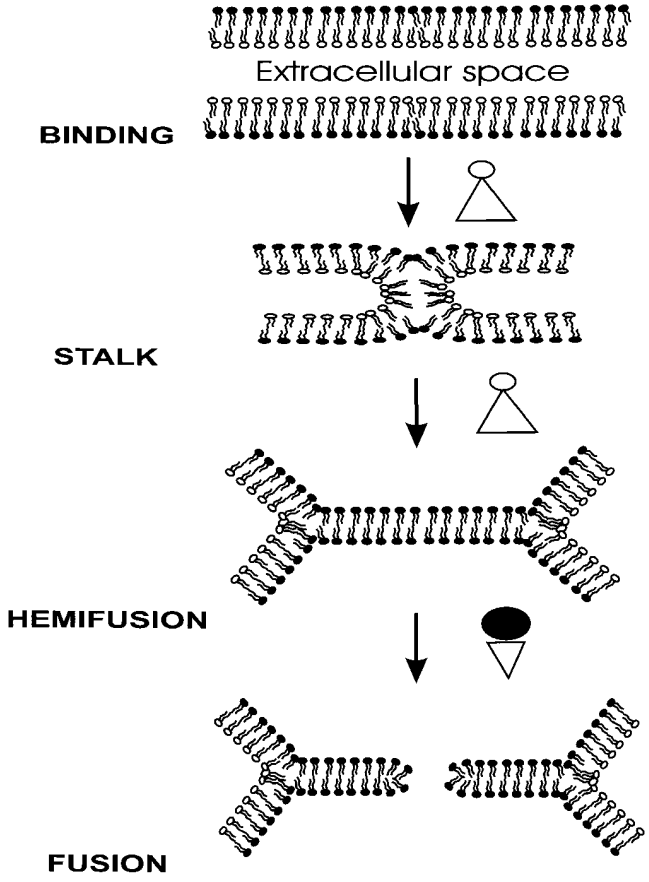

Figure 1. Schematic representation of fusion progressing from a bound state to membranes connected by a stalk, followed by stalk expansion to form an HD, and then to pore formation that completes fusion. The lipids curve in opposite directions for the stalk and pore. A cone-shaped agent (as shown) facilitates formation of a stalk. Inverted cone-shaped, positive curvature agents (shown between hemifusion and fusion) inhibit formation of a stalk but promote formation of a pore within the HD. The HD is composed of cytoplasmic leaflets of both cells and separates the aqueous compartments of the two fusing cells.

leaflets to form stalks, but also for lipids in inner leaflets to reorient into a fusion pore within an HD (Chernomordik et al., 1987; Kozlov et al., 1989) (Fig. 1, *fusion*). A pore in an HD (Fig. 1, *fusion*) has net positive curvature. Thus, inverted cone-shaped agents would, upon inserting in the inner leaflets, promote pore formation; cone-shaped agents, when in the inner leaflets, would inhibit pore formation. This expectation of the stalk-pore hypothesis has been verified in pure lipidic fusion systems (Chernomordik et al., 1987; Kozlov et al., 1989). LPC acting on distal leaflets has been shown to promote pore formation in an HD that connects two bulged planar bilayer membranes (Chernomordik et al., 1987) and in an HD that connects a liposome to a planar membrane (Chernomordik et al., 1995*c*). The role of lipid shape of distal leaflets in promoting the transition from hemifusion to fusion has not, until now, been experimentally tested for protein-mediated fusion because a system demonstrating hemifusion was not available and because of the technical difficulty of gaining access to the inner monolayers.

Cells expressing the ectodomain of HA that is glycosylphosphatidylinositol (GPI)–linked to outer leaflets (GPI-HA) have been shown to hemifuse, but do not fuse, to RBCs (Kemble et al., 1994; Melikyan et al., 1995*b*). The cytoplasmic compartments of hemifused cells remain separated by a stable HD. We have found a means to overcome the problem of how to gain access to the inner monolayers by using membrane-permeable amphipaths that are surface active and insert into inner leaflets of RBCs and other cells (Seeman, 1972; Sheetz and Singer, 1974; Browning and Nelson, 1976; Steck, 1989). Exogenous amphipathic agents were selected to modify the external and/or cytoplasmic leaflets of plasma membranes of hemifused cells to test the role of the different leaflets in fusion pore formation. Using GPI-HA–mediated hemifusion as an experimental model, we have been able to demonstrate that increases in the positive curvature of inner monolayers promote correspondingly more pore formation within an HD.

Amphipathic agents that preferentially partitioned into the external leaflets of cell membranes, such as methochlorpromazine (M-CPZ), did not promote fusion pore formation. In contrast, membrane-permeable, cationic amphipaths (MPCAs), such as chlorpromazine, partitioned into cytoplasmic leaflets and caused formation of fusion pores within the hemifusion diaphragm between GPI-HA cell–RBC pairs. We show that MPCAs lower the energy for forming pores in phospholipid bilayers. This is consistent with MPCAs promoting fusion by rendering the spontaneous curvature of cytoplasmic leaflets of plasma membranes more positive, as predicted by the stalk-pore hypothesis (Kozlov et al., 1989). We also characterize connections between pairs of RBCs and cells expressing wild-type HA when membrane, but not aqueous, probes redistribute. We show that these connecting structures are different from the diaphragms between RBCs and GPI-HA–expressing cells.

Materials and Methods

Chemicals and Solutions

Dioleoylphosphatidylcholine (DOPC), dioleoylphosphatidylethanolamine (DOPE), bovine brain phosphatidylserine (PS), lyso-lauroylphosphatidylcholine (L-LPC), and lyso-stearoylphosphatidylcholine (S-LPC) were purchased from Avanti Polar Lipids, Inc. (Alabaster, AL) and used as received. Oleic acid, arachidonic acid, and defatted BSA were obtained from Sigma Chemical Co. (St. Louis, MO). Chlorpromazine (CPZ), trifluoperazine (TFP), dibucaine (DB), trinitrophenol, dipyridamole, and squalene were from Aldrich Chemical Co. (Milwaukee, WI). M-CPZ was a generous gift of Smith Kline Beecham Pharmaceuticals (King of Prussia, PA). Solutions with amphipaths, at the indicated concentrations, were prepared freshly just before experiments and stored in the dark. All fluorescent dyes: 6-carboxyfluorescein (CF), octadecylrhodamine B chloride (R18), NBD-taurine (NBD-t), and tetramethylrhodamine-labeled dextran (mol wt 40,000) were purchased from Molecular Probes (Eugene, OR).

HA-expressing Cells

All HA-expressing cell lines were received from J.M. White (University of Virginia, Charlottesville). CHO cells transfected with X:31 influenza HA (HA300a cell line referred to as WT cells) or with engineered GPI-linked ectodomain of HA (referred to as GPI cells) were maintained as described (Kemble et al., 1994) in a glutamate-deficient medium supplemented with 400 μM L-methionine sulfoximine (Sigma Chemical Co.), 250 μM 1-deoxymannojirimycin (Calbiochem-Novabiochem Corp., San Diego, CA), and defined calf serum (Hyclone Laboratories, Inc., Logan, UT).

Labeling of RBCs with Lipidic and Aqueous Dyes and Video Microscopy

Fresh human RBCs, obtained from the Rush Blood Gas Laboratory, were loaded with 1–2.5 mM CF by mild hypotonic lysis (Ellens et al., 1989) and labeled with the lipidic dye R18 essentially according to Morris et al. (1989). Typically, only ~70% of the RBCs became loaded with CF; all of them were labeled by R18. To monitor fusion pore enlargement, separate batches of RBCs were colabeled with CF and a large aqueous marker, rhodamine-dextran (RD), using the same mild hypotonic lysis protocol as described above. CF and RD were dissolved in a loading solution to a final concentration of 1 mM and 0.2 mM, respectively. Both dyes were efficiently trapped in the RBCs after resealing. To study the fusion of HA-expressing cells to intact RBCs, RBCs were loaded with NBD-t (Sarkar et al., 1989). RBCs were labeled just before the experiment and stored on ice for no longer than 6 h.

Fusion of HA-expressing cells to RBCs was monitored under an upright microscope with fluorescence attachment (Leitz D, Edison, NJ) using a ×20 or ×40 ELWD objective (Nikon Inc., Garden City, NY). Standard rhodamine (for R18, RD) or fluorescein (for CF, NBD-t) filter sets were used to visualize the spatial redistribution of membrane and aqueous dyes upon hemifusion and/or fusion. Fluorescence images were obtained by a videocamera (SIT-66; DAGE MTI, Indianapolis, IN) and recorded on VHS format videotape. Selected frames from the tape were digitized off-line by a frame grabber (Meteor; Matrox Electronic System, Ltd., Quebec, Canada).

Hemifusion and Fusion of RBCs to HA-expressing Cells

HA-expressing cells were grown to 30–40% confluency and made fusion competent, and RBCs were bound as described (Melikyan et al., 1995*b*). Hemifusion/fusion between HA-expressing cells and RBCs was triggered at room temperature by exposing them to a pH 4.9 solution for 2 min and reneutralizing with a pH 7.4 solution supplemented with 2 mg/ml glucose as a metabolic substrate. Cells were incubated at room temperature for the indicated period of time (usually 4–5 min) before examining the redistribution of the fluorescent dye under the microscope. A fusion index was calculated for each dish by randomly selecting several areas and normalizing the number of HA-expressing cells stained with a given dye by the total number of cells decorated with at least one RBC. About 200 cells were screened for each dish.

To determine the effects of the amphipaths on redistribution of membrane and aqueous fluorescent dyes after hemifusion or fusion was triggered, cells were exposed to these agents for 1 min (in the dark), and then washed once with solutions free of drug. 20–50 mM raffinose (Sigma Chemical Co.) was included in the solutions to compensate for the osmotic pressure of the hemoglobin in RBCs, thereby eliminating possible swelling of RBCs that might lead to transfer of aqueous dye (Melikyan et al., 1995*b*). The amphipaths had previously been dissolved in PBS containing raffinose that was made isotonic and the pH was adjusted to 7.0. The presence of raffinose did not affect the transition from hemifusion to fusion for intact RBCs, but slightly lowered the fusion index for ghosts (not shown). The same fusion indices were obtained when stachyose or dextran (mol wt 10,000) was substituted for raffinose. This demonstrates that aqueous dye transfer was caused by direct action of the amphipaths on the HD or on small fusion pores, not by concomitant cell swelling. R18 facilitated pore enlargement: a smaller percentage of wild-type (WT) cells were stained by CF when the RBCs were not labeled with R18. Therefore, for studies quantifying transfer of CF and/or RD, RBCs were not labeled by R18. Unless otherwise stated, experiments were carried out at room temperature.

Experiments with Planar Lipid Bilayers

Solvent-free planar phospholipid bilayers were formed on an ~250-μm hole from a solution of DOPE/DOPC/PS (6:3:1 wt/wt) in squalene. The voltage-clamped membranes were bathed by a 150 mM NaCl, 10 mM Tris buffer, pH 7.0, solution containing 1 mM ascorbic acid, 1 mM sodium sulfite, and 1 mM sodium bisulfite to prevent oxidation of CPZ during experiments. The specific capacitance was calculated as the measured membrane capacitance divided by the area of the hole. The bilayer tension (σ) was calculated from the increment in its area (measured by the increase in capacitance) that resulted from application of hydrostatic pressure differences between the two bathing solutions (Sukharev et al., 1982). This technique was verified by independently measuring with a stereo microscope the area increment of a bulged bilayer formed on a conical Teflon partition in response to hydrostatic pressures (Tien, 1974). Both methods gave similar results. We routinely used the electrical technique because it is more convenient.

The line tension of the lipidic pore (γ) was calculated using a technique based on dielectric breakdown of the bilayer. The dependence of the lifetime (τ) of the membrane on the applied voltage (V) can be described by (Abidor et al., 1979)

$$\tau = A\exp\{\pi\cdot\gamma^2/[kT(\sigma + C_m(\varepsilon_w/\varepsilon_m - 1)V^2/2)]\}, \quad (1)$$

where A is a preexponential factor that is independent of voltage; $\epsilon_w = 80$ and $\epsilon_m = 2$ are the dielectric constants of water and of the hydrophobic core of the membrane, respectively; C_m is the specific membrane capacitance; k is the Boltzmann constant; T is temperature in °K; and π has its usual numerical meaning. A and γ were determined by nonlinear curve-fitting (SigmaPlot; Jandel Scientific, San Rafael, CA) the above equation to the experimental dependence of the bilayer lifetime on voltage (Chernomordik et al., 1987, 1994). To measure this dependence, voltage pulses of varying amplitude were applied to planar bilayers, and the times from application of the pulse to the fast and irreversible increase in current across the bilayer were measured (on average, 10 experiments for each voltage).

Results

Complete Fusion of Stably Hemifused Cells Is Induced by Modification of the Inner but Not Outer Leaflets

Fig. 2 shows a typical fluorescence pattern observed after GPI cells and RBCs were induced to hemifuse by transiently lowering pH. The membrane dye (*R18*) redistributed between cells (Fig. 2, *A* and *B*), while the aqueous dye (*CF*) remained within RBCs (Fig. 2, *C* and *D*), consistent with hemifusion (Melikyan et al., 1995*b*). Subsequent application of 0.5 mM CPZ for 1 min resulted in a fast redistribution of the aqueous dye (Fig. 2 *E*) without altering the fluorescence pattern of the already spread R18. Likewise, addition of other MPCAs—trifluoperazine and dibucaine—to hemifused cells resulted in fast aqueous dye redistribution (i.e., in fusion, see Fig. 3 *A*). (While we typically present data for CPZ in this paper, equivalent results were obtained with TFP and DB at their appropriate concentrations.) A similar effect of MPCAs was observed when GPI cells were hemifused to intact RBCs loaded with NBD-t (not shown). The cells had to be hemifused for these agents to promote fusion. In control experiments, fusion was not observed when cationic amphipaths were applied to cell–RBC pairs not exposed to acidic pH or when pH was lowered but HA0 was not cleaved into its fusion-competent HA1–HA2 form (not shown). In contrast to the case of MPCAs partitioned into inner leaflets, treatment of hemifused cells with agents that preferentially or exclusively partitioned into outer monolayers—such as M-CPZ (Fig. 2 *F*), L-LPC, trinitrophenol, dipyridamole, oleic acid, and arachidonic acid—did not result in a transition from hemifusion to fusion. Even at slightly lytic concentrations of these compounds, CF from ghosts or NBD-t from intact RBCs did not redistribute. Thus, agents did not promote fusion when inserted in outer leaflets, independent of whether they conferred positive (LPC; Epand, 1985) or negative (oleic and arachidonic acid; Hope and Cullis, 1981; Epand et al., 1991) curvature.

The MPCAs induced fusion of hemifused cell pairs in a concentration-dependent fashion (Fig. 3 *A*). When RBCs

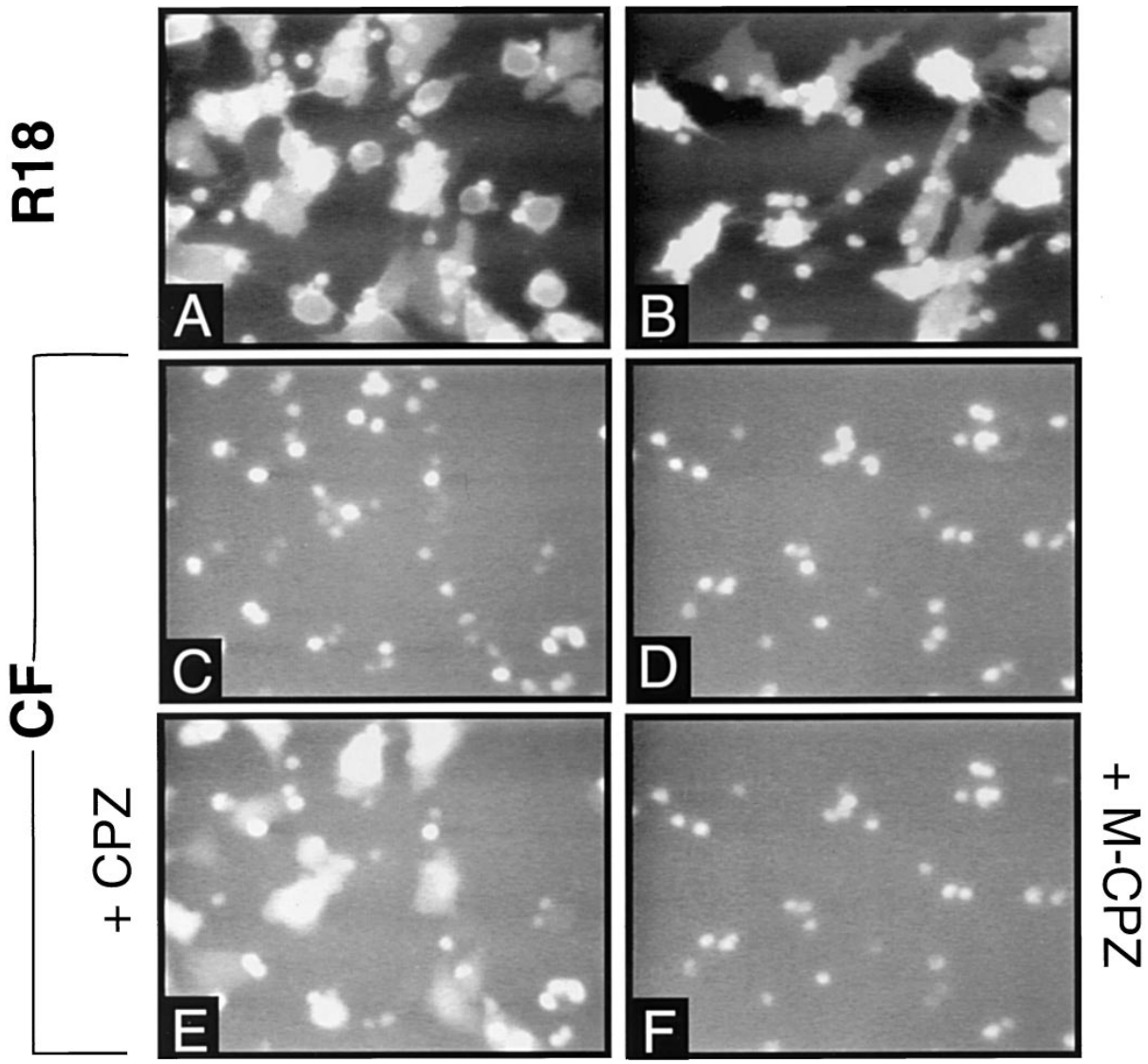

Figure 2. Chlorpromazine induces complete fusion between hemifused GPI cells and RBCs. RBCs were colabeled with CF and R18. 5 min after fusion was triggered by a brief exposure of cell–RBC pairs to an acidic pH, the redistribution of R18 between RBCs and GPI cells was completed (*A* and *B*), whereas CF did not spread into the GPI cells (*C* and *D*). Transiently (for 1 min) exposing cells in the left-hand panels to 0.5 mM CPZ resulted in efficient CF redistribution without detectable lysis (*E*, compare with *C*). In contrast, similar treatment of cells shown in the righthand panels with 1 mM of membrane-impermeable M-CPZ did not lead to any changes in CF fluorescence pattern (*F*, same as *D*). The CPZ did not cause a redistribution of R18, but it did strongly quench the R18 fluorescence in a concentration-dependent fashion.

loaded with either CF or NBD-t were hemifused to GPI-expressing cells, increasing concentrations of phenothiazines or local anesthetics resulted in a higher extent of fusion. The creation of pores was confined to the HD: the aqueous dye transferred into as much as 90% of the GPI cells decorated by RBCs, without a significant lytic release of dye into the external solution. The relative efficiencies of TFP, CPZ, and DB in inducing full fusion correlated well with their pharmacological potency and ability to cause hemolysis (Seeman, 1972).

At low pH, agents with a tertiary amine, such as CPZ, exist predominantly in their membrane-impermeable charged form and are kinetically trapped within the external leaflets. Fusion was not detected when hemifused cell pairs were treated with CPZ at pH 4.9 for 1 min. However, the transition from hemifusion to full fusion increased when the cell pairs were incubated with 0.4 mM CPZ for 1 min at higher pH values before removing the drug (Fig. 3 *B*). Deprotonated CPZ in the external leaflet translocated into the inner leaflet where it promoted fusion; this was validated by comparing the dye transfer to the ratio of the deprotonated to protonated form of CPZ as a function of pH , using pK_{CPZ} 9.3 (Perrin, 1965) (Fig. 3 *B*, *solid line* and *righthand scale*). The extent of fusion correlated well with the fraction of the neutral, nonprotonated form of CPZ. Both CPZ at low pH and M-CPZ at all pH values partitioned into the external leaflet of membrane where they did not induce the hemifusion-to-fusion transition. In short, full fusion was observed only when CPZ had access to the cytoplasmic leaflets.

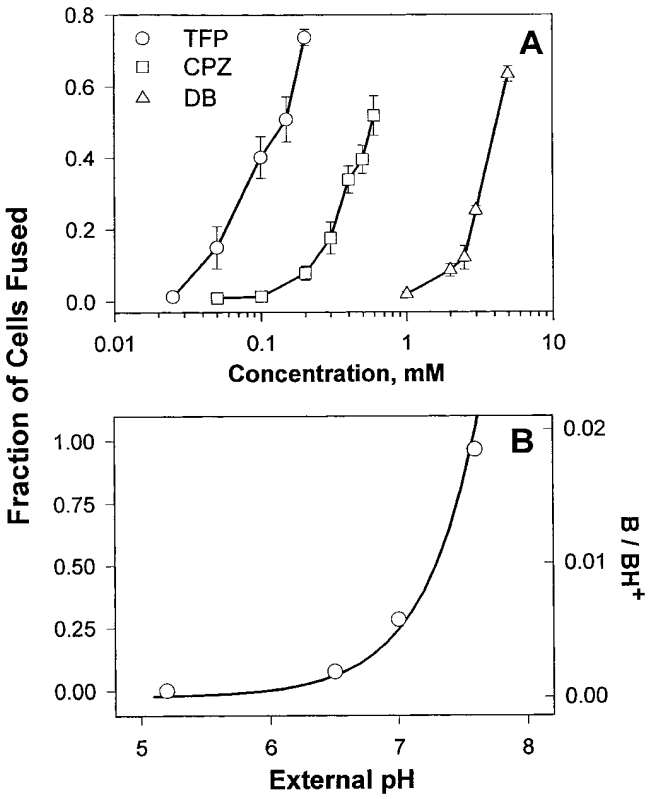

Figure 3. (*A*) Concentration dependence of hemifusion-to-fusion transition induced by phenothiazines (*CPZ* and *TFP*) and a local anesthetic (*DB*). The fusion efficiency at pH 7.0 was calculated as the ratio of cells stained with NDB-t to the total number of cells decorated with RBCs. The functional forms of extent of fusion vs concentration (note semilogarithmic scale) were similar for all three drugs, despite the differences in effective concentration ranges. Error bars show the standard errors for four to eight experiments. (*B*) Efficiency of hemifusion-to-fusion transition induced by CPZ as a function of pH. GPI cells hemifused to RBCs were briefly exposed to 0.4 mM CPZ buffered at the indicated pH values. Cells were returned to a CPZ-free solution at the same pH, and the fraction of cells stained with NBD-t was counted (*circles*, *lefthand scale*). The standard error was smaller than the size of the symbols. The ratios of the neutral (*B*, membrane-permeable) and protonated (BH^+) forms of CPZ were calculated assuming pK 9.3 and are shown by the solid line (*righthand scale*).

Membrane-permeable Cationic Drugs Promote Formation of Pores in Planar Lipid Bilayers

In the hemifusion state, lipids of the outer leaflets are free to move from one cell membrane to the other, whereas lipids of the inner leaflets remain confined to their original cells. Integral membrane proteins should not be able to pass through the junction where the two cell membranes and the HD meet (Fig. 1, *hemifusion*) without disrupting the HD. These proteins should remain confined to their original membrane, excluded from the HD. Since we conjecture that the HD is devoid of integral membrane proteins, we envision that the mechanism of pore formation within an HD could be identical to that of pure lipid bilayers (Fig. 1, *fusion*). Therefore, the physical chemical mechanism by which CPZ and the other amphipaths destabilize the hemifusion diaphragm was explored by investigating their effects on planar lipid bilayers. Voltages applied across the bilayer facilitate the formation and enlargement of lipid pores in bilayers (Abidor et al., 1979), resulting in irreversible breakdown: once a lipidic pore exceeds a critical radius in a planar membrane, it enlarges indefinitely in the microsecond time scale. Line tension, the energy per unit length of the edge of a pore, imposes a contracting force. Line tension arises, in large part, because lipid monolayers are bent into highly curved hydrophilic pores in a bilayer. Micelle-forming lipids, such as LPC, readily insert into the circumference of the highly curved pore (Fig. 1, fusion) and lower its line tension (Chernomordik et al., 1987). Such lipids therefore reduce the contracting force and thereby decrease the mean lifetime, τ, of a bilayer at a given applied voltage.

In the presence of 1 mM CPZ or 4 mM DB added to both sides of the membrane (Fig. 4, *filled diamonds* and *filled squares*, respectively), lower voltages were required to cause irreversible breakdown than in the absence of these drugs (*filled circles*). The line tension of the pore, γ, was estimated by curve-fitting the theoretical equation for electrical breakdown (Eq. 1) to experimental data. γ decreased from 16.0 $\pm$ 1.0 pN for a bilayer not exposed to drugs to 3.7 $\pm$ 0.2 and 4.1 $\pm$ 0.6 pN in the presence of CPZ and DB, respectively. Thus, the partitioning of cationic drugs into the planar bilayer lowered the energetic barrier for lipidic pore formation and enlargement. This parallels the action of the amphipaths on HDs connecting hemifused GPI cell–RBC pairs. Lowering of γ by MPCAs in an HD would facilitate lipid arrangement into the highly curved pore and thus would account for their ability to induce the hemifusion-to-fusion transition. The lowering of γ and facilitation of pore formation also provides a possible mechanism by which high concentrations of CPZ and DB promote hypotonic lysis of RBCs (Seeman, 1972). Adding a lower concentration of CPZ (0.1 mM, *open diamonds*) to the membrane did not appreciably affect the line tension of the pore (17.1 $\pm$ 0.4 pN). This low concentration of CPZ was also not efficient in inducing fusion of stably hemifused cell pairs (Fig. 3 *A*).

Somewhat higher concentrations of MPCAs were required to substantially lower the line tension of lipidic pores in bilayers than to induce the hemifusion-to-fusion transition. The need for higher concentrations with bilayers may simply reflect the differences in experimental systems. Addition of 1 mM CPZ (but not 0.1 mM) or 4 mM DB to one or both sides of preformed bilayers inevitably led to their breakdown within a few seconds in the absence of an applied voltage. This indicates that the drugs destabilized the bilayer during their initial incorporation, before they reached equilibrium between the membrane, aqueous phase, and torus that connects the bilayer to the Teflon partition. This breakdown is probably analogous to the destabilization of the HD in hemifused cell pairs. Bilayers that were reformed in the presence of these drugs were sufficiently stable to allow their lifetimes to be measured as a function of voltage (Fig. 4).

Suboptimal Fusion Conditions Lead to Transfer of Membrane but Not Aqueous Dyes from RBCs to WT Cells

The extent and rate of fusion increase with higher surface density of HA (Ellens et al., 1990; Clague et al., 1991; Me-

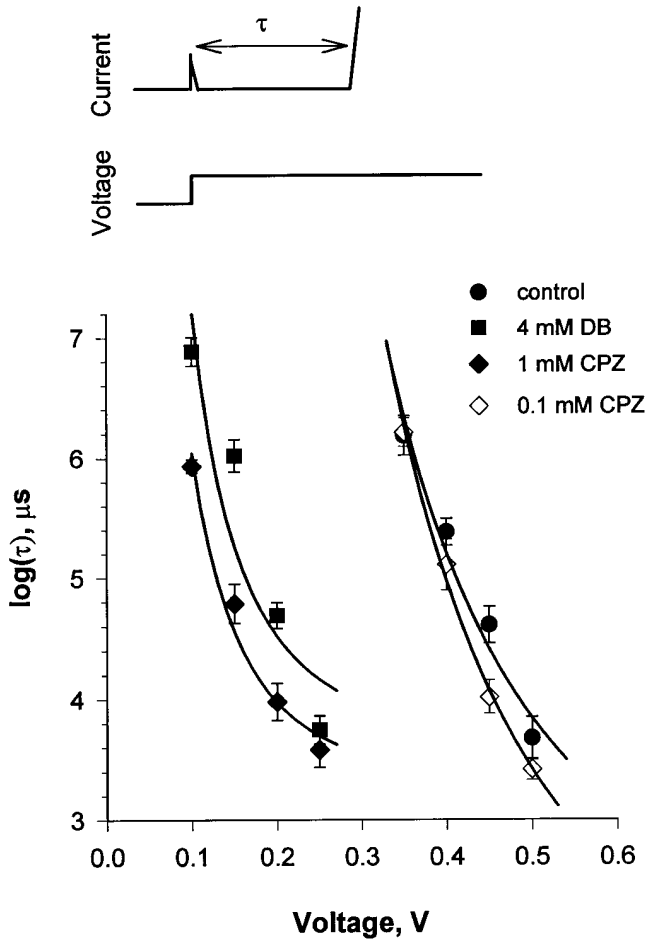

Figure 4. The effect of CPZ and DB on the propensity of lipids to form a pore in planar lipid bilayers. (*Upper panel*) Schematic illustration of the current (*top trace*) upon application of a voltage step (*bottom trace*) that results in irreversible breakdown of a planar membrane. The lifetime of the planar bilayer (τ) is defined as the time from stepping to a given voltage to the moment of the irreversible increase of current signifying membrane breakdown. (*Lower panel*) Semilogarithmic plot of τ as a function of applied voltage (*V*). Standard errors are shown for 10–12 experiments. The line tensions of lipidic pores were estimated by curve-fitting (*solid lines*) Eq. 1 to experimental data. The specific capacitance, C_m, and surface tension, σ, of DOPE/DOPC/PS bilayers were measured in the absence (*control*) and presence of amphipathic agents. $C_m = 0.66 \pm 0.05$ μF/cm^2 was not affected by the agents, but $\sigma = 0.42 \pm 0.04$ mN/m was lowered significantly by 1 mM CPZ or 4 mM DB to 0.21 ± 0.02 and 0.15 ± 0.03 mN/m, respectively. $\sigma = 0.36 \pm 0.04$ mN/m in the presence of 0.1 mM CPZ was not appreciably lower than control. (*Filled circles*) Control, γ = 16.0 pN ($R^2 = 0.96$); (*open diamonds*) 0.1 mM CPZ, γ = 17.1 pN ($R^2 = 0.99$); (*filled squares*) 4 mM dibucaine, γ = 4.1 pN (R^2 = 0.85); (*filled diamonds*) 1 mM CPZ, γ = 3.7 pN ($R^2 = 0.98$).

likyan et al., 1995*a*; Danieli et al., 1996), higher temperature (Stegmann et al., 1990), and lower pH over a narrow range below the fusion threshold (Wharton et al., 1986). For example, the kinetics of R18 transfer is slower at room temperature (22–23°C) than at 37°C (Morris et al., 1989). At room temperature the majority of WT cells became stained by R18 within a few min of triggering fusion (Fig. 5, *A* and *B*), whereas the aqueous dye (CF) transferred into only a small fraction of the cells (Fig. 5, *C* and *D*). The fraction of cells labeled with aqueous dye increased with time after fusion was triggered. However, even 30 min after reneutralization, less than half of the WT cells with bound RBCs received CF (data not shown). The WT cells stained by R18 but not CF may have hemifused to RBCs or may have become connected by small and/or transient fusion pores that did not allow passage of a detectable amount of aqueous dye (Zimmerberg et al., 1994). Raising the temperature to 37°C promoted transfer of CF without appreciably increasing spread of R18, which was already high. We refer to the situation where wild-type HA promotes easy spread of membrane dye but poor transfer of aqueous dye as "stunted fusion."

CPZ Enlarges Fusion Pores between RBCs and WT Cells but Only Forms Small Pores between Hemifused RBCs and GPI Cells

As was the case with GPI cells (Fig. 2), MPCAs promoted transfer of CF in stunted fusion. However, almost an order of magnitude lower concentration of drug was required to promote aqueous dye transfer from RBCs to WT cells than to GPI cells (see below). For example, ~0.1 mM CPZ greatly facilitated the transfer of CF from RBCs to WT cells (Fig. 5 *E*). In contrast, 1 mM of the impermeant M-CPZ did not promote transfer of CF, although washing out the M-CPZ caused some dye transfer (Fig. 5 *F*, *arrow*). The mechanism by which this removal promoted CF redistribution is not clear.

We assessed the average size of CPZ-induced pores by coloading RBCs with CF and a larger aqueous marker RD (mol wt 40,000) (Schoch and Blumenthal, 1993). These RBCs were bound to either WT cells or GPI cells, and fusion/hemifusion was triggered at room temperature. Neither dye spread from RBCs into GPI cells, consistent with a hemifusion phenotype (not shown). For WT, 5 min after acidification, few cells were stained by CF (Fig. 6 *A*) and were rarely labeled by RD (Fig. 6 *B*). A low concentration of CPZ (0.1 mM) resulted in substantial transfer of CF (Fig. 6 *C*). This was accompanied by RD movement into some WT cells (Fig. 6 *D*, *arrowhead*). More cells became stained by both CF and RD with 0.5 mM CPZ (Fig. 6, *E* and *F*). The transfer of RD clearly shows that relatively large pores resulted from the CPZ treatment, either by growth of previously existing pores or formation and enlargement of new pores. Much higher concentrations of CPZ were required to induce CF and RD transfer between hemifused GPI–RBC pairs. However, even at high concentrations of CPZ, the large marker, RD, did not move into GPI cells as well as it did into WT cells (see below).

The transfer of CF and RD into cells was quantified by plotting the percentage of cells stained by these dyes vs CPZ concentrations (Fig. 7). CPZ was much more efficient in promoting transfer of both dyes from RBC to WT cells (Fig. 7 *B*) than to GPI cells (Fig. 7 *A*). Also, CF transfer increased with CPZ concentration up to 0.7 mM for GPI cells, whereas it saturated for WT cells with $K_{1/2} \sim$ 0.025 mM. The relative size of fusion pores was characterized by plotting the ratio of cells stained with RD to those that acquired CF as a function of CPZ concentration. The RD/CF ratios were independent of the CPZ concentration between 0.1 and 0.7 mM when hemifused GPI cell–RBC

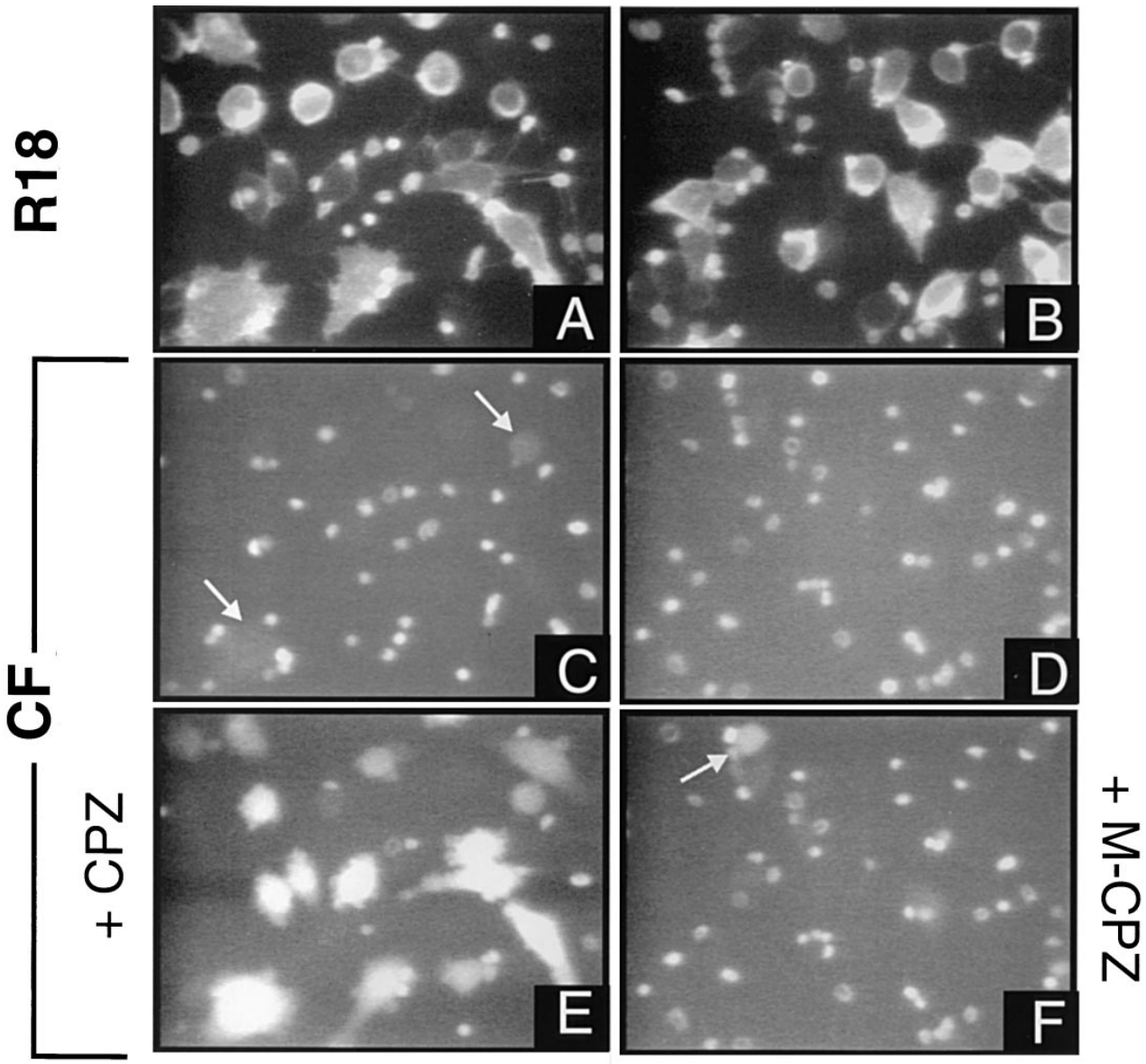

Figure 5. The transfer of membrane and aqueous dye between CF/R18-colabeled RBCs and WT cells. R18 redistributed efficiently between cells upon transient exposure to low pH (*A* and *B*), but only a small amount of CF (*C* and *D*) transferred into only a few cells (*arrows*) 5 min after reneutralization. A transient (1-min) exposure to 0.1 mM CPZ induced substantial amounts of CF to transfer to almost all the WT cells (*E*). There was additional spread of R18 during the time between *A* and *E* (not shown). In contrast, treatment with 1 mM M-CPZ did not lead to full fusion, although washing it out induced some CF transfer (*F*, *arrow*) by an unknown mechanism.

pairs were treated with CPZ (Fig. 7 *C*, *filled circles*). In contrast, the RD/CF ratio increased with CPZ concentration for WT cells (Fig. 7 *C*, *filled squares*). This suggests that for WT cells larger fusion pores became more probable in the presence of higher concentrations of CPZ. For GPI cells, CPZ promotes pore formation, but the size distribution does not appear to increase with greater concentrations of CPZ. Thus, MPCAs at low concentrations promote large pores in stunted fusion, whereas, even at high concentrations, they promote relatively small pores in HDs.

LPC in Outer Leaflets Inhibits Formation of Pores by MPCAs in Stable Hemifusion Diaphragms but Does Not Alter the Effect of MPCAs in Stunted Fusion

Placing LPC into external leaflets of hemifused cell membranes strongly inhibited the ability of MPCAs to induce the hemifusion-to-fusion transition (Fig. 8). When CPZ alone was added (i.e., as a control, LPC was not added), the majority of GPI cells became stained by CF (Fig. 4, *lefthand bar*).[2] However, pretreating the hemifused cells with 5 μM S-LPC dramatically inhibited the hemifusion–fusion transition induced by application of 0.3 mM CPZ,

2. CPZ was more efficient in promoting aqueous dye redistribution between RBCs and GPI cells in these experiments than in the experiment of Fig. 3 *A*. For Fig. 3 *A*, NBD-t–loaded RBCs were treated with 4,4′-diisothiocyanato-stilbene-2,2′-disulfonic acid (DIDS; Sigma Chemical Co.) to prevent leakage of NBD-t (Sarkar et al., 1989). However, DIDS treatment inhibited R18 redistribution (not shown) and was omitted in this series of experiments to avoid possible interference with LPC or CPZ.

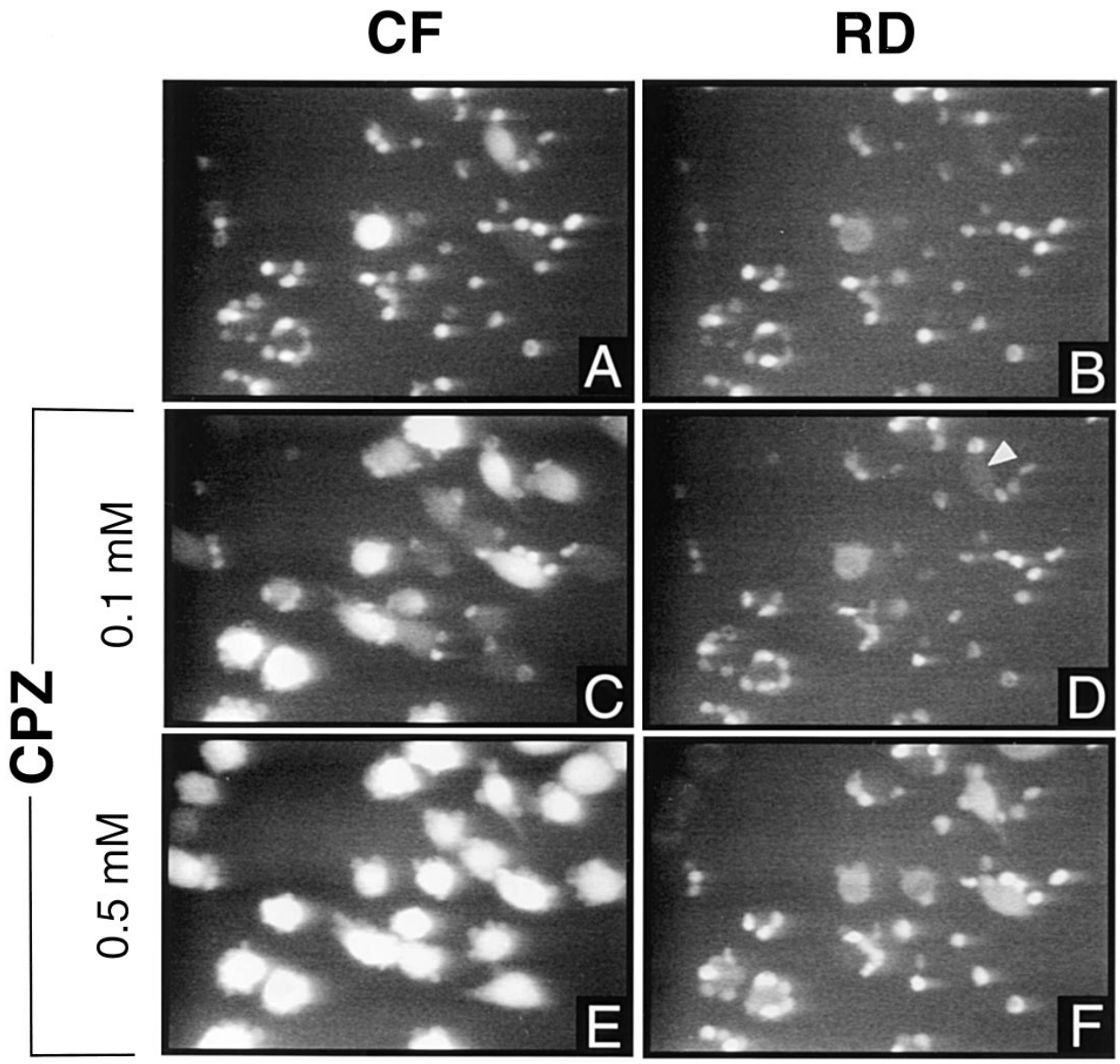

Figure 6. The extent of transfer of small (*CF*) and large (*RD*) aqueous probes between RBCs and WT cells. Within 5–10 min after fusion was triggered, a few cells were stained by CF (*A*), whereas only a rare cell was stained by RD (*B*). Even 30 min after acidification, a substantial fraction (about one-half) of the WT cells were stained with CF, whereas virtually all the RD was still confined to RBCs (not shown). A brief (1-min) exposure to 0.1 mM CPZ dramatically increased the transfer of CF (*C*), but only slightly facilitated the spread of RD (*D*, *arrowhead*). Subsequent transient treatment of these cells with 0.5 mM CPZ resulted in virtually complete spread of CF (*E*) and significantly higher transfer of RD (*F*). The fluorescence of CF was brighter after CF spread into WT cells (compare *C* and *E* to *A*): RD probably quenched CF fluorescence within RBCs by resonance energy transfer.

even when the S-LPC in solution was removed by washing (Fig. 8, *middle bar*). The destabilizing effect of CPZ on the hemifusion diaphragm was completely eliminated by treating the cells with 20 μM S-LPC (not shown). We used S-LPC (rather than a shorter chained L-LPC or M-CPZ) because it neither flip-flops nor desorbs from the external leaflet of membrane after washing out unincorporated S-LPC on the time scale of our experiment (Chernomordik et al., 1993). Thus, by using S-LPC, we avoided possible interaction between the external leaflet agent and CPZ in bulk solution through micellization or other processes. Removing the adsorbed S-LPC by adding delipidated BSA restored the destabilizing effect of CPZ (Fig. 8, *righthand bar*). The fact that incorporating agents into external leaflets inhibited the action of agents on inner leaflets is consistent with the state of the outer leaflet affecting the action of agents on the hemifusion diaphragm (see Discussion).

Differences between stunted fusion and hemifusion were demonstrated by the action of membrane-impermeant amphipaths on transfer of aqueous dye. After the fusion protocol, treatment of WT–RBC pairs with membrane-impermeant amphipaths (e.g., 1 mM M-CPZ or 0.17 mM L-LPC) for 1 min did not facilitate CF redistribution (not shown), but, in contrast with the GPI cells, removal of

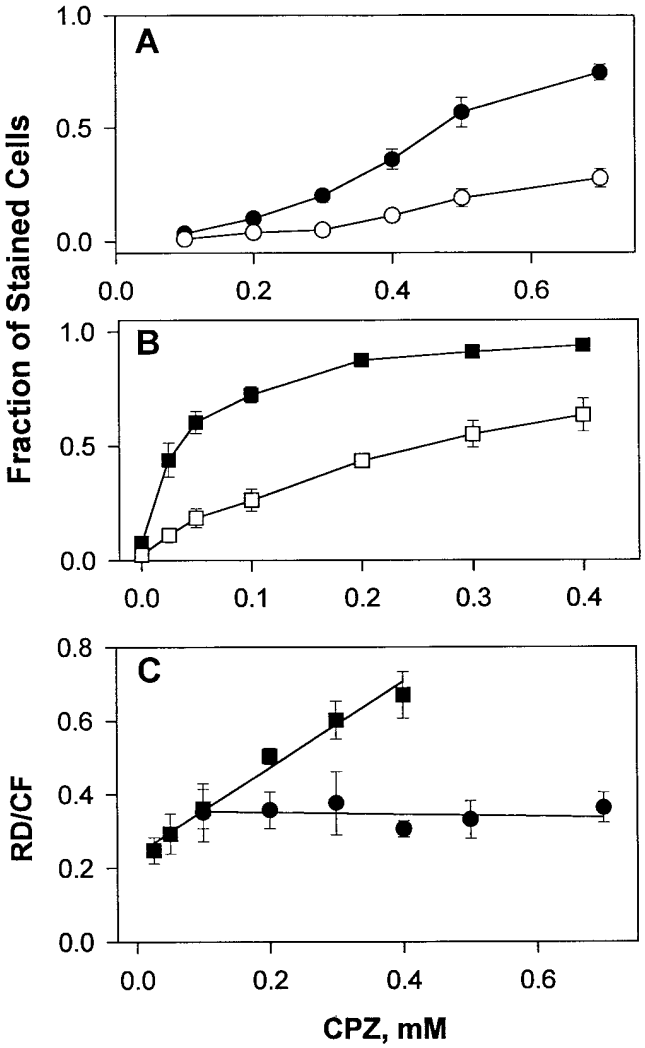

Figure 7. Transfer of a small (*CF*, *filled symbols*) and large (*RD*, *open symbols*) probe from RBCs to GPI (*A*, *circles*) and WT cells (*B*, *squares*) as a function of CPZ concentration 5 min after reneutralizaion. These results are replotted as the ratio of WT (*squares*) and GPI (*circles*) cells stained with RD to those stained with CF vs CPZ concentration (*C*). Error bars represent standard errors of three to seven independent experiments.

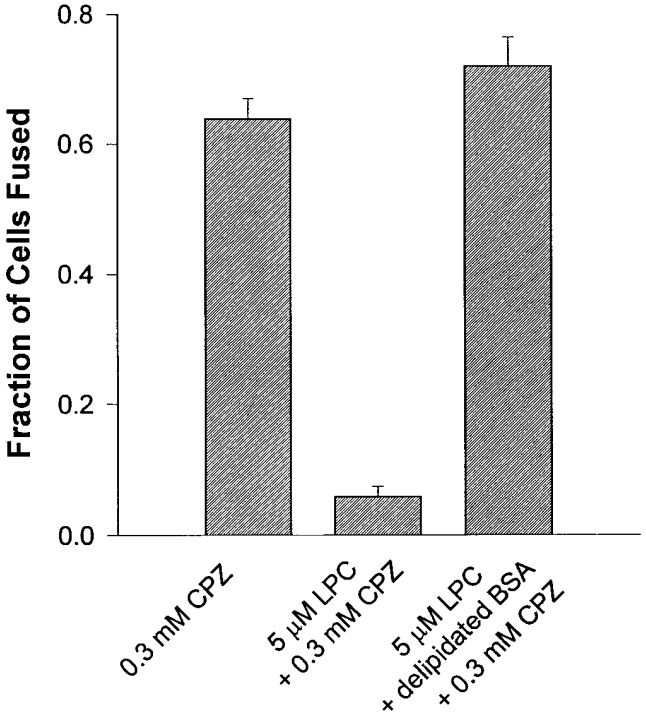

Figure 8. LPC incorporated into external leaflets of hemifused cells inhibits CPZ-induced fusion. The fraction of cells stained with NBD-t after exposure to 0.3 mM CPZ is shown (*lefthand bar*). Preincubation of hemifused cell pairs with 5 μM S-LPC for 2 min followed by washing out unincorporated S-LPC resulted in a strong inhibition of complete fusion induced by a subsequent application of 0.3 mM CPZ (*middle bar*). When S-LPC was removed from the external leaflets by incubating the cells with 4 mg/ml of delipidated BSA for 5 min before CPZ treatment, the extent of fusion was restored (*righthand bar*). Standard errors are shown for three experiments.

the amphipaths from the external leaflets by washing with an agent-free solution induced some CF transfer (Fig. 5 *F*, *arrow*). Another difference between stunted fusion and hemifusion is that treatment of WT–RBC pairs with 20 μM S-LPC did not inhibit the redistribution of CF induced by 0.1 mM CPZ (not shown). In contrast, pretreatment of GPI–RBC pairs with S-LPC protected the HD against the action of CPZ (Fig. 8). Thus, the action of the amphipaths is clearly different for hemifusion induced by GPI-HA and the stunted fusion mediated by wild-type HA. Stunted fusion was also observed with HAb2 cells (a cell line expressing higher densities of HA than WT cells [Ellens et al., 1990]) when fusion was triggered with suboptimal conditions: room temperature rather than 37°C. Low concentrations of CPZ promoted pore enlargement with these cells in the same described manner.

Discussion

We have used amphipathic agents that insert into either inner or outer leaflets to evaluate how altering the curvature of each of the monolayers affects formation of fusion pores after stable hemifusion between GPI cells and RBCs. MPCAs induced pore formation when they were introduced into inner leaflets of hemifused cells and therefore into HDs. When inserted into outer leaflets, amphipaths did not promote aqueous dye spread. This study demonstrates that positive spontaneous curvatures of inner leaflets promote pore formation within an HD. Also, these agents promoted aqueous dye transfer when inserted within inner leaflets of cell pairs that exhibited stunted fusion.

The high concentrations of amphipaths, however, undoubtedly alter more than spontaneous monolayer curvatures. One can therefore argue that other altered properties account for our results. For example, the micelle-forming agents when acting on inner leaflets that constitute the HD may destabilize it by extracting lipids. Or the amphipaths may interact with cytoskeletal proteins or with integral membrane proteins excluded from the HD. But the effects of MPCAs on purely lipidic bilayers are consistent with formation of positive curvature lipidic pores. The the-

ory of spontaneous monolayer curvature and how it is altered therefore provides a simple, unified, and non–ad hoc explanation for our fusion and bilayer breakdown data.

MPCAs Can Selectively Destabilize Hemifusion Diaphragms

CPZ and DB when inserted into lipid bilayers have been directly shown to confer positive spontaneous curvatures and inhibit H_{II}-phase formation (Hornby and Cullis, 1981). TFP, along with CPZ and DB, exhibit phenomena expected of positive curvature amphipaths: they have high critical micelle concentrations (MacDonald, 1986; Binford and Palm, 1994) and lower the energy of pores in lipid bilayers (Fig. 4). At low concentrations, the partition coefficient of CPZ from aqueous solution into membranes is roughly 3,000 (Lieber et al., 1984). At equilibrium, CPZ could thus constitute as much as 50% of the membrane lipid for 1 mM in solution. However, significantly less amphipath probably inserted into membranes in our experiments. Equilibrium may not have been reached for the 1-min incubation with CPZ (the drug was incubated for several hours to measure the partition coefficient). Also, the partitioning of CPZ and M-CPZ into membranes saturates with increasing aqueous concentration (Zachowski and Durand, 1988).

With long times of incubation, MPCAs are lytic at the concentrations we used (Seeman, 1972; Lieber et al., 1984). By exposing hemifused cell pairs to MPCAs only briefly, however, lipidic pores subsequently formed in only the HD without causing cell lysis. The most likely explanation for selective targeting to the HD is that the agents preferentially accumulated within inner monolayers. This accumulation causes MPCAs to be present in both leaflets of the HD; these agents are therefore at a higher concentration than in the plasma membrane where they reside in only a single leaflet.

Preferential accumulation of material into one leaflet of a cell membrane creates mismatches in area between the two leaflets. According to the well-documented "bilayer couple hypothesis," the resulting stresses are relieved by membrane bending toward the leaflet with excess material (Sheetz and Singer, 1974; Browning and Nelson, 1976; Steck, 1989). In other words, accumulation of material into inner leaflets of RBCs causes their membranes to bend inward into cup shapes; accretion of molecules into outer leaflets causes the RBCs to crenate outward. The MPCAs are cup-formers whereas M-CPZ and LPC are crenating agents (Deuticke, 1968; Sheetz and Singer, 1974). Even if MPCAs did not preferentially partition into inner leaflets, the fraction of the membrane-permeable amphipaths that did do so promoted the hemifusion-to-fusion transition: membrane-impermeant agents that only partition into outer leaflets, such as M-CPZ and LPC, did not promote the hemifusion-to-fusion transition. Also, the percentage of cell pairs undergoing the transition correlated with the fraction of CPZ in the neutral membrane-permeable form.

In the case of stunted fusion, LPC did not inhibit the ability of CPZ to promote aqueous dye spread. This shows that LPC, per se, does not prevent CPZ from reaching inner leaflets. In contrast, LPC in outer monolayers protects the HD from destabilization by CPZ (Fig. 8). We offer a possible explanation: before hemifusion, the region of contact between two cells consists of inner and outer leaflets. After hemifusion, material of the outer monolayer has been "pushed" out of the region it formerly occupied that is now occupied only by the HD. Since there is conservation of material in the inner and outer leaflets, the material of the outer monolayers becomes compressed relative to that of the inner monolayers. This mismatch in areas becomes more accentuated as the HD enlarges, and it should limit the size of the HD, assuming the mismatch is not relieved by lipid flip-flop. Insertion of LPC into outer monolayers would further increase the compression of these leaflets. Compression would be relieved by a shrinking of the HD. If the addition of LPC significantly reduced the area of the HD, CPZ could be rendered ineffective in destabilizing the small HD because the probability of forming a pore should be proportional to the area of the HD. If this explanation is correct, the size of an HD can be experimentally manipulated.

MPCAs Can Be Used to Distinguish Stable Hemifusion from Stunted Fusion

We found conditions under which CF did not spread from RBCs to WT cells, but R18 did. While this pattern of dye movement is that of hemifusion, several lines of evidence show that the structure that hinders aqueous dye from transferring in stunted fusion is distinctly different from the stable hemifusion intermediate induced by GPI-HA. Notably, the effective concentrations of CPZ and TFP required to promote aqueous dye redistribution between RBCs and WT cells were substantially lower than those required for GPI cells. Also, the average size of the fusion pore connecting WT cells to RBCs could be gradually enlarged by increasing the concentration of CPZ. In contrast, for GPI cells, more pores formed within an HD with increasing CPZ concentration, but average pore size did not change (Fig. 7, *A* and *C*). This is reminiscent of the action of CPZ on RBC membranes. By measuring sieving of two different size molecules, it was concluded that increased CPZ concentration generated additional, but not larger, pores (Lieber et al., 1984). The pores created by CPZ in the lipidic HD and in the protein-containing plasma membrane of RBCs may be fundamentally the same. It appears to be energetically more favorable for increased concentrations of CPZ to create new pores in membranes rather than to enlarge the small pores already generated by the amphipath.

The structures in stunted fusion are either partially weakened HDs (weakened perhaps by limited insertion of the transmembrane domain) and/or fusion pores that remain small for long periods of time (Tse et al., 1993; Zimmerberg et al., 1994). If they are HDs, this would provide strong evidence that hemifusion is a bona fide intermediate of full fusion because improved conditions (e.g., lower pH or higher temperature) induce transfer of aqueous dye. The membrane-active MPCAs may promote and/or enlarge pores by making the spontaneous curvature of inner leaflets more positive or by interacting with the transmembrane domain of HA. If the latter is true, it would indicate that HA is part of the fusion pore and, in addition to inducing pore formation, is important in pore enlargement.

For topological reasons, the transmembrane domain of HA should normally be excluded from the HD. Therefore, any tendency for the domain to be driven into the HD as a result of conformational changes of HA should tend to destabilize the HD (Melikyan et al., 1995*b*). In this circumstance, fusion pores would be protein–lipid complexes (Zimmerberg et al., 1991) rather than purely lipidic structures. Lipids and proteins could then act synergistically to enlarge pores: the insertion of the transmembrane domain into the HD could coax the spontaneous curvature of the inner leaflets to become more positive and to promote the formation of fusion pores.

We are grateful to Dr. Judith White for providing us with the HA-expressing cell lines, to Smith Kline Beecham Pharmaceuticals for the generous gift of methochlorpromazine, and to the Rush Blood Gas Lab for supplying us with fresh RBCs. We thank Drs. Leonid Chernomordik and Yvonne Lange for valuable suggestions on the manuscript.

This work was supported by National Institutes of Health grant GM27367.

Received for publication 16 September 1996 and in revised form 27 November 1996.

References

Abidor, I.G., V.B. Arakelian, L.V. Chernomordik, Yu.A. Chizmadzhev, V.F. Pastushenko, and M.R. Tarasevich. 1979. Electrical breakdown of BLM: main experimental facts and their qualitative discussion. *Bioelectrochem. Bioenerg.* 6:37–52.

Binford, J.S., Jr., and W.H. Palm. 1994. Adsorption of surfactants by membranes: erythrocytes versus synthetic vesicles. *Biophys. J.* 66:2024–2028.

Browning, J.L., and D.L. Nelson. 1976. Amphipathic amines affect membrane excitability in *Paramecium*: role of bilayer couple. *Proc. Natl. Acad. Sci. USA.* 73:452–456.

Chernomordik, L.V., G.B. Melikyan, and Yu. A. Chizmadzhev. 1987. Biomembrane fusion: a new concept derived from model studies using two interacting planar lipid bilayers. *Biochim. Biophys. Acta.* 906:309–352.

Chernomordik, L.V., S.S. Vogel, E.A. Leikina, A. Sokoloff, H.O. Onoran, and J. Zimmerberg. 1993. Lysolipids reversibly inhibit Ca^{2+}-, GTP- and pH-dependent fusion of biological membranes. *FEBS Lett.* 318:71–76.

Chernomordik, L.V., A.N. Chanturia, E. Suss-Toby, E. Nora, and J. Zimmerberg. 1994. An amphipathic peptide from the C-terminal region of the Human Immunodeficiency Virus envelope glycoprotein causes pore formation in membranes. *J. Virol.* 68:7115–7123.

Chernomordik, L.V., M.M. Kozlov, and J. Zimmerberg. 1995*a.* Lipids in biological membrane fusion. *J. Membr. Biol.* 146:1–14.

Chernomordik, L.V., E. Leikina, M.-S. Cho, and J. Zimmerberg. 1995*b.* Control of Baculovirus gp64-induced syncytium formation by membrane lipid composition. *J. Virol.* 69:3049–3058.

Chernomordik, L.V., A. Chanturia, J. Green, and J. Zimmerberg. 1995*c.* The hemifusion intermediate and its conversion to complete fusion: regulation by membrane composition. *Biophys. J.* 69:922–929.

Clague, M.J., C. Schoch, and R. Blumenthal. 1991. Delay time for influenza virus hemagglutinin-induced membrane fusion depends on hemagglutinin surface density. *J. Virol.* 65:2402–2407.

Danieli, T., S.L. Pelletier, Y.I. Henis, and J.M. White. 1996. Membrane fusion mediated by the influenza virus hemagglutinin requires the concerted action of at least three hemagglutinin trimers. *J. Cell Biol.* 133:559–569.

Deuticke, B. 1968. Transformation and restoration of biconcave shape of human erythrocytes induced by amphipathic agents and changes in ionic environment. *Biochim. Biophys. Acta.* 163:494–500.

Ellens, H., S. Doxsey, J.S. Glenn, and J.M. White. 1989. Delivery of macromolecules into cells expressing a viral membrane fusion protein. *Methods Cell Biol.* 31:155–176.

Ellens, H., J. Bentz, D. Mason, F. Zhang, and J.M. White. 1990. Fusion of influenza hemagglutinin-expressing fibroblasts with glycoprotein-bearing liposomes: role of hemagglutinin surface density. *Biochemistry.* 29:9697–9707.

Epand, R.M. 1985. Diacylglycerols, lysolecithin, or hydrocarbons markedly alter the bilayer to hexagonal phase transition temperature of phosphatidylethanolamines. *Biochemistry.* 24:7092–7095.

Epand, R.M., R.F. Epand, N. Ahmed, and R. Chen. 1991. Promotion of hexagonal phase formation and lipid mixing by fatty acids with varying degrees of unsaturation. *Chem. Phys. Lipids.* 57:75–80.

Günter-Ausborn, S., A. Praetor, and T. Stegmann. 1995. Inhibition of influenza-induced membrane fusion by lysophosphatidylcholine. *J. Biol. Chem.* 270:29279–29285.

Hope, M.J., and P.R. Cullis. 1981. The role of nonbilayer lipid structures in the fusion of human erythrocytes induced by lipid fusogens. *Biochim. Biophys. Acta.* 640:82–90.

Hornby, A.P., and P.R. Cullis. 1981. Influence of local and neutral anaesthetics on the polymorphic phase preferences of egg yolk phosphatidylethanolamine. *Biochim. Biophys. Acta.* 647:285–292.

Kemble, G.W., T. Danieli, and J.M. White. 1994. Lipid-anchored influenza hemagglutinin promotes hemifusion, not complete fusion. *Cell.* 76:383–391.

Kozlov, M.M., S.L. Leikin, L.V. Chernomordik, V.S. Markin, and Yu.A. Chizmadzhev. 1989. Stalk mechanism of membrane fusion. *Eur. Biophys. J.* 17: 121–129.

Lieber, M.R., Y. Lange, R.S. Weinstein, and T.L. Steck. 1984. Interaction of chlorpromazine with the human erythrocyte membrane. *J. Biol. Chem.* 259: 9225–9234.

MacDonald, R.I. 1986. Trifluoperazine inhibits Sendai virus-induced hemolysis. *Biochim. Biophys. Acta.* 856:337–347.

Melikyan, G.B., W.D. Niles, and F.S. Cohen. 1995*a.* The fusion kinetics of influenza hemagglutinin expressing cells to planar bilayer membranes is affected by HA density and host cell surface. *J. Gen. Physiol.* 106:783–802.

Melikyan, G.B., J.M. White, and F.S. Cohen. 1995*b.* GPI-anchored influenza hemagglutinin induces hemifusion to both red blood cell and planar bilayer membranes. *J. Cell Biol.* 131:679–691.

Morris, S.J., D.P. Sarkar, J.M. White, and R. Blumenthal. 1989. Kinetics of pH - dependent fusion between 3T3 fibroblasts expressing influenza hemagglutinin and red blood cells. *J. Biol. Chem.* 264:3972–3978.

Perrin, D.D. 1965. Dissociation Constants of Organic Bases in Aqueous Solution. Butterworths, London. 366 pp.

Sarkar, D.P., S.J. Morris, O. Eidelman, J. Zimmerberg, and R. Blumenthal. 1989. Initial stages of influenza hemagglutinin-induced cell fusion monitored simultaneously by two fluorescent events: cytoplasmic continuity and lipid mixing. *J. Cell Biol.* 109:113–122.

Schoch, C., and R. Blumenthal. 1993. Role of the fusion peptide sequence in initial stage of influenza hemagglutinin-induced cell fusion. *J. Biol. Chem.* 268:9267–9274.

Seddon, J.M. 1990. Structure of the inverted hexagonal (H_{II}) phase, and non-lamellar phase transitions of lipids. *Biochim. Biophys. Acta.* 1031:1–69.

Seeman, P. 1972. The membrane action of anesthetics and tranquilizers. *Pharmacol. Rev.* 24:583–655.

Shangguan, T., D. Alford, and J. Bentz. 1996. Influenza virus-liposome lipid mixing is leaky and largely insensitive to the material properties of the target membrane. *Biochemistry.* 35:4956–4965.

Sheetz, M.P., and S.J. Singer. 1974. Biological membranes as bilayer couples. A molecular mechanism of drug-erythrocyte interactions. *Proc. Natl. Acad. Sci. USA.* 71:4457–4461.

Siegel, D.P. 1993. Modeling protein-induced fusion mechanisms: insight from the relative stability of lipidic structures. *In* Viral Fusion Mechanisms. J. Bentz, editor. CRC Press, Inc., Boca Raton, FL. 475–512.

Steck, T.L. 1989. Red cell shape. *In* Cell Shape: Determinants, Regulation, and Regulatory Role. W.D. Stein and F. Bronner, editors. Academic Press, Inc., San Diego, CA. 205–246.

Stegmann,T., J.M. White, and A. Helenius. 1990. Intermediates in influenza induced membrane fusion. *EMBO (Eur. Mol. Biol. Organ.) J.* 9:4231–4241.

Sukharev, S.I., L.V. Chernomordik, I.G. Abidor, and Yu.A. Chizmadzhev. 1982. Effects of UO_2^{2+} ions on the properties of bilayer lipid membranes. *Bioelectrochem. Bioenerg.* 9:133–140.

Tien, H.Ti. 1974. Bilayer Lipid Membranes: Theory and Practice. Marcel Dekker, New York. 532 pp.

Tilcock, C.P.S., and P.R. Cullis. 1987. Lipid polymorphism. *Ann. NY Acad. Sci.* 492:88–102.

Tse, F.W., A. Iwata, and W. Almers. 1993. Membrane flux through the pore formed by a fusogenic viral envelope protein during cell fusion. *J. Cell Biol.* 121:543–552.

Vogel, S.S., E.A. Leikina, and L.V. Chernomordik. 1993. Lysophosphatidylcholine reversibly arrests exocytosis and viral fusion at a stage between triggering and membrane merger. *J. Biol. Chem.* 268:25764–25768.

Wharton, S.A., J.J. Skehel, and D.C. Wiley. 1986. Studies of influenza haemagglutinin-mediated membrane fusion. *Virology.* 149:27–35.

White, J.M. 1992. Membrane fusion. *Science (Wash. DC).* 258:917–924.

Zachowski, A., and P. Durand. 1988. Biphasic nature of the binding of cationic amphipaths with artificial and biological membranes. *Biochim. Biophys. Acta.* 937:411–416.

Zimmerberg, J., M. Curran, and F.S. Cohen. 1991. A lipid/protein complex hypothesis for exocytotic fusion pore formation. *Ann. NY Acad. Sci.* 635:307–317.

Zimmerberg, J., R. Blumenthal, D.P. Sarkar, M. Curran, and S.J. Morris. 1994. Restricted movement of lipid and aqueous dyes through pores formed by influenza hemagglutinin during cell fusion. *J. Cell Biol.* 127:1885–1894.